A Sliding Mode Based Damping Control of DFIG for Interarea Power Oscillations

Kai Liao, Zhengyou He, *Senior Member, IEEE*, Yan Xu, *Member, IEEE*, Guo Chen, *Member, IEEE*, Zhao Yang Dong, *Senior Member, IEEE*, and Kit Po Wong, *Fellow, IEEE*

***Abstract*—This paper proposes a second-order sliding mode-based damping controller of DFIG for interarea oscillations. The proposed damping control strategy aims to utilize the reactive power modulation ability of DFIG to stabilize the power system in the event of oscillations caused by disturbances. First, the proposed controller is derived based on a two-area power system, and then it is extended to multiarea power systems. Compared with the conventional damping controller, the proposed one is insensitive to modeling uncertainties and parameter variations. Given the wide variation of operation points, the proposed sliding mode-based damping controller demonstrates a better robustness than the conventional damping controller. Simulation results on a two-area power system and a 10-machine 39-bus power system with DFIG-based wind farm integration show the improvement on system performance in interarea oscillation damping and demonstrate the robustness of the proposed control scheme in a wide operation region.**

***Index Terms*—DFIG, second-order sliding mode, interarea oscillation, damping control.**

I. Introduction

WIND power has been rapidly integrated into modern power grids. It is expected that the growing trend will continue in the following decades to alleviate the energy shortage and environmental pressure [1]. Among the various wind power generators, doubly fed induction generator (DFIG) have accounted for a large market due to their advantages of relatively small size, low power rating of the back-to-back power electronic converters, high energy efficiency and the capability of flexible control [2], [3]. Thus, the DFIG based wind farms will play an important role in today's and future power system operation.

On the other hand, as the size of the inter-connected power system grows, technical problems such as interarea oscillation have been reported, which is a critical threat for the stability of power system operation [4], [5]. As ref. [6] shows, the integration of large-scale DFIG wind farm may have negative impacts on power system rotor angle stability. For the system with high penetration of DFIGs, the advanced power electronic convertors in DFIG can be utilized to damp the power system oscillations with increased flexibility. Over the past few years, several damping control techniques for DFIGs have been studied to increase the system damping [7]- [16]. In [7], a conventional damping controller, which is similar to the power system stabilizer (PSS) installed on a synchronous generator, was designed for DFIG to improve the system dynamic response. [8] introduced a damping controller for DFIG based on the root locus analysis, which is used for interarea oscillation damping enhancement. The optimization method is also employed to coordinate the parameters of the damping controller for DFIG in [15]. In [17] and [18], the intelligent algorithms were employed to improve the system dynamic response. In fact, both active and reactive power modulation of DFIG can provide damping contribution. The study in [19] has shown that reactive power modulation of DFIG for damping control is an alternative choice, because the active power modulation may cause shaft oscillation.

However, these damping controllers for DFIG are designed based on the small signal linearization algorithm with respect to one fixed operation point. But the operation status of power systems are varying from time to time. Thus, these methods may not be robust to the model parameters and the system operation point uncertainties. Given the uncertain and random changes in system states, the controller may not be able to sustain the stability of the system.

This paper aims to develop a new robust damping controller of DFIG against system uncertainties and parameter variations based on the sliding mode control algorithm. This algorithm is insensitive to system uncertainties and parameter variations. This method provides new prospect for dealing with increasing uncertainties. The sliding mode control has several promising characteristics. Fox example, the designed controllers are relatively simple, easy to implement and low computational burden required. Compared to designing techniques based on system linearization, the designing procedure of the sliding mode control is capable of dealing with several kinds of internal and external disturbances, model uncertainties, and operation point changing. The first-order sliding mode control technique has

Manuscript received January 15, 2016; revised March 29, 2016 and June 24, 2016; accepted July 19, 2016. Date of publication August 2, 2016; date of current version December 14, 2016. This work was supported in part by the International Cooperation Project supported by Sichuan Provincial Science and Technology Department under Grant 2015HH0055, in part by Australian Research Council Discovery Scheme under Grant DE160100675, and in part by China Southern Power Grid Research under Grant WYKJ00000027. Paper no. TSTE-00048-2016 *(Corresponding author: Guo Chen)*.

K. Liao is with the Department of Electrical Engineering, Southwest Jiaotong University, Chengdu 610031, China, and also with the School of Electrical and Information Engineering, The University of Sydney, Sydney, NSW 2006, Australia (e-mail: liaokai.lk@foxmail.com).

Z. He is with the Department of Electrical Engineering, Southwest Jiaotong University, Chengdu 610031, China (e-mail: hezy@home.swjtu.cn).

Y. Xu and Z. Dong are with the Department of Electrical and Information Engineering, The University of Sydney, Sydney, NSW 2006, Australia (e-mail: yanxuee@hotmail.com; joe.dong@sydney.edu.au).

G. Chen is with the School of Electrical Engineering and Computer Science, The University of Newcastle, Callaghan, NSW 2308, Australia (e-mail: guochen@ieee.org).

K. P. Wong is with the School of Electrical, Electronic, and Computer Engineering, the University of Western Australia, Crawley, WA 6009, Australia (e-mail: Kitpo@ieee.org).

Color versions of one or more of the figures in this paper are available online at http://ieeexplore.ieee.org.

Digital Object Identifier 10.1109/TSTE.2016.2597306

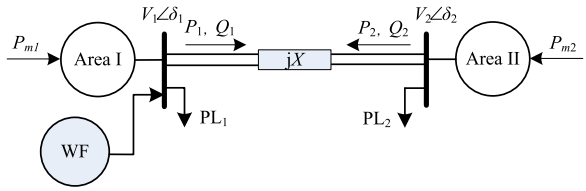

Fig. 1. Diagram of the two-area power system with wind farm integration.

been used to damp the interarea power oscillations for multi-area power systems in [20], which is based on the reactive power control of SVC. However, the first-order sliding mode control requires the discrete control action and it is impractical for the DFIG to generate discrete reactive power output.

In order to address the issues mentioned above, this paper proposes a second-order sliding mode based interarea oscillation damping controller for DFIG. This method utilizes the flexible reactive power modulation ability of DFIG to damp power oscillations and successfully avoids the requirement of a discrete reactive power output. The advantages of the proposed second-order sliding mode damping control lie in the high degree of robustness to the wide operation point variation and in the smoothness of the control action. It is important to note that the proposed damping controller is insensitive to the unmodeled system dynamics. The proposed sliding mode based damping controller is firstly introduced for a classic two-area power system, and then, the designing method is implemented to a multi-area power system. The simulations on two-area power system and 10-machine 39-bus system show the effectiveness of the proposed second-order sliding mode damping controller in damping interarea power system oscillations.

The remaining of this paper is organized as follows: Section II describes the background of interarea oscillation problem. Section III presents the designing progress of the proposed sliding mode based damping controller for a two-area power system. Section IV introduces the implementation of a multi-area power system. Simulation results and detailed discussion are presented in Section V. Section VI gives the conclusion.

II. Brief Description of Intereara Oscillations in Wind Farm Integrated Power System

A two-area power system with wind generation [8]–[10], as shown in Fig. 1, is considered in this section to illustrate the interarea oscillation. The two areas, each with a local load, are connected through a double AC transmission line. In this study, the DFIG based wind farm is integrated at area I. A fixed shunt capacitive compensator is also connected at the same bus with wind farm.

The dynamic model of the two-area power system without wind generation connection can be described using the swing equation as shown in (1), which is widely used in [21]– [23].

$$\begin{aligned}\dot{\delta}_{12} &= \omega_{12}\\ \dot{\omega}_{12} &= \frac{1}{H_1}(P_{m1}-P_{L1}) - \frac{1}{H_2}(P_{m2}-P_{L2})\\ &\quad - \left(\frac{1}{H_1}+\frac{1}{H_2}\right)\frac{V_1}{V_2}\sin\delta_{12}\end{aligned} \tag{1}$$

where δ represents the generator rotor angle and ω represents the generator rotor speed. δ_{12} and ω_{12} are the relative rotor angle and relative rotor speed between the two areas, respectively, with $\delta_{12}=\delta_1-\delta_2$ and $\omega_{12}=\omega_1-\omega_2$. The reactance X is the total impedances of the double circuit AC transmission line. H_1 and H_2 represent the equivalent inertia of area I and area II, respectively. In (1), the damping coefficient of synchronous machine is not considered. However, for the sliding mode damping control designing, the damping coefficient is considered in the uncertain part.

When the wind farm is linked to area I, as illustrated in Fig. 1, the system dynamic behavior can be described as

$$\begin{aligned}\dot{\delta}_{12} &= \omega_{12}\\ \dot{\omega}_{12} &= \frac{1}{H_1}(P_{m1}+P_w-P_{L1}) - \frac{1}{H_2}(P_{m2}-P_{L2})\\ &\quad - \left(\frac{1}{H_1}+\frac{1}{H_2}\right)\frac{V_1}{V_2}\sin\delta_{12}\end{aligned} \tag{2}$$

where P_w is the active power generated from the wind farm.

In the above system, the transmitted active power is relevant to the angle difference between the two areas. The transmitted reactive power from area I to area II is relevant to the magnitude of the voltage. In other words, the voltage magnitude will be influenced by the transmitted reactive power with the relationship given in Eq.(3). The power swing damping can be improved by modulating the bus voltage via reactive power control [24].

$$Q_1 = Q_w + Q_{s0} = \frac{V_2^2 - V_1V_2\cos\delta_{12}}{X} \tag{3}$$

where Q_1 is the reactive power transmitted from area I to area II. Q_w is the reactive power injection of DFIG, and Q_{s0} is the reactive power generated by fixed shunt capacitive compensators and synchronous generators.

It is known that the generators operate synchronously in the two areas under the steady-state conditions. The relative angle δ_{12} remains constant, and the relative rotor speed ω_{12} keeps zero. However, in case of disturbance, unbalance between generator electrical and mechanical powers is created, leading to the power oscillation between the two areas. For the system stability concerns, such oscillation should be damped quickly. In this paper, the second-order sliding mode control algorithm based damping controller is designed to damp the system interarea oscillation via modulating the reactive power of DFIG based wind farm.

III. Sliding Mode Based Damping Controller Design

In this section, the sliding mode based damping control strategy for DFIG integrated into a two-area power system is presented. The second-order sliding mode is applied to design the damping controller for DFIG in this paper.

A. Sliding Variable Selection

The purpose of the second-order sliding mode control algorithm is to zero the selected sliding variable σ and its first time derivative $\dot{\sigma}$. The sliding variable is selected based on the desired control objectives, to guarantee the control achievement when

$\sigma = 0$. In this study, damping the power oscillation is meant to keep the relative angle between the two areas as a constant. In other words, it is to maintain the relative rotor speed ω_{12} with the value of zero. Thus, the sliding variable σ can be chosen as $\sigma = \omega_{12}$.

Among the several second-order sliding mode algorithms, the twisting algorithm [25], [26] has a quite simple law of control action, and thus the trajectories can reach sliding surface in a finite time. Furthermore, another advantage of the twisting algorithm is in the wider range of operation and the algorithm does not markedly increase the implementation of complexity. This implies that the computational burden should be low during the online operation of the controller.

B. Damping Controller Design

For the two-area power system, choosing the power angle $\delta_2 = 0$ as the reference angle, the system dynamics can be rewritten as

$$\begin{aligned}\dot{\delta} &= \omega_{12}\\ \dot{\omega}_{12} &= \frac{1}{H_1}(P_{m1} - P_{L1}) - \frac{1}{H_2}(P_{m2} - P_{L2})\\ &\quad - \left(\frac{1}{H_1} + \frac{1}{H_2}\right)\frac{V_1}{V_2}\sin\delta. \end{aligned} \tag{4}$$

Using the modulated variable Q_w (the reactive power of DFIG), and utilizing the relationship shown in (3) so as to substitute the voltage of bus 1, the system swing equation can be rewritten as

$$\begin{aligned}\dot{\omega}_{12} &= \frac{1}{H_1}(P_{m1} - P_{L1}) - \frac{1}{H_2}(P_{m2} - P_{L2})\\ &\quad - \left(\frac{1}{H_1} + \frac{1}{H_2}\right)\left(\frac{\sin\delta}{X\cos\delta}V_2^2 - \frac{\sin\delta}{\cos\delta}(Q_w + Q_{s0})\right). \end{aligned} \tag{5}$$

In this study, the modulation of the output reactive power of DFIG based wind farm, Q_w, is used to damp the interarea oscillation. The sliding mode control requires a discrete control action. However, the output reactive power of DFIG can not change suddenly. Thus, the output reactive power of DFIG cannot be used as a control action directly.

The reactive power control scheme of DFIG is shown in Fig. 2. The reactive power is usually modulated via a two-loop PI controller, i.e. outer reactive power loop and inner current loop [27], respectively. As shown in Fig. 2, the Q_{ref} can be the actual control action for sliding mode damping control. However, if the full mode of the reactive power control loop is considered, the relative degree will be large. Thus, the damping controller designing will use a high order derivation, which will be much more difficult. Otherwise, the dynamic behavior of the reactive power control loop can be similarly represented by a first-order inertia loop. On the other hand, the designed sliding model control performs well on the robustness to the bounded unmolded part. The adopted first-order inertia loop for the equivalent of

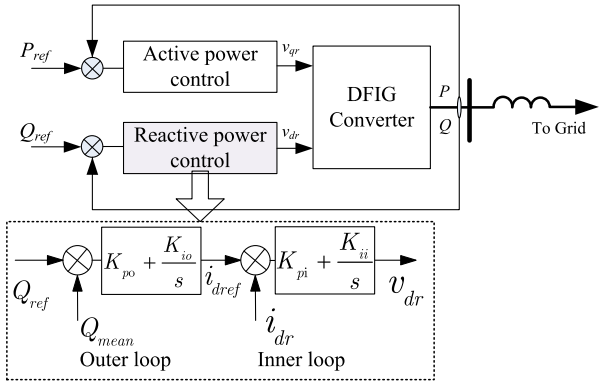

Fig. 2. The reactive power control scheme of DFIG.

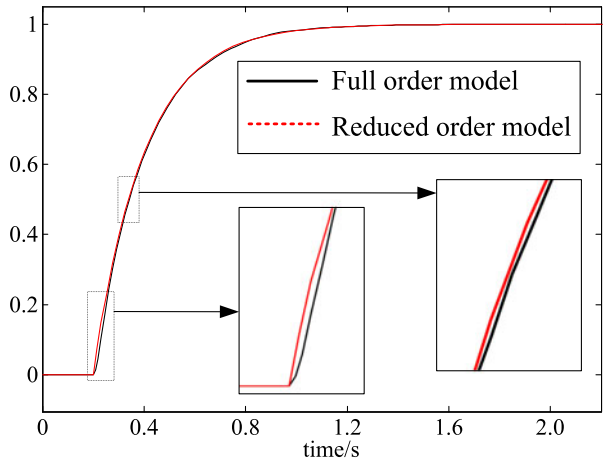

Fig. 3. Step response of full order reactive power loop and reduced order reactive power loop of DFIG.

reactive power control loop is shown as

$$\Delta Q_w = \frac{\Delta Q_{ref}}{sT + 1}. \tag{6}$$

The dynamic behaviors of full order model system and the equivalent first-order inertia loop(with $T = 0.2$s) for a step response are compared in Fig. 3 (the parameters of DFIG is given in Appendix). It is shown that the dynamic behavior (step response) of equivalent first-order inertia response is similar to the one of full order model system.

As the dynamic behavior of DFIG reactive power control loop is obtained, the whole system dynamic equations can be represented as

$$\begin{aligned}\dot{\delta} &= \omega_{12}\\ \dot{\omega}_{12} &= \frac{1}{H_1}(P_{m1} - P_{L1}) - \frac{1}{H_2}(P_{m2} - P_{L2})\\ &\quad - \left(\frac{1}{H_1} + \frac{1}{H_2}\right)\frac{\sin\delta}{\cos\delta}\left(\frac{V_2^2}{X} - \Delta Q_w - Q_w - Q_{s0}\right)\\ \Delta\dot{Q}_w &= \frac{u - \Delta Q_w}{T} \end{aligned} \tag{7}$$

where u is the additional reactive power part (ΔQ_{ref}) used for damping control. Q_w is the rated reactive power of wind farm under nominal operation. Thus, the output reactive power of wind farm is $Q_w + \Delta Q_w$.

Eq.(7) shows that the relative degree of the selected sliding variable ($\sigma = \omega_{12}$) is 2, with

$$\begin{aligned}\ddot{\omega}_{12} &= \left(\frac{1}{H_1}+\frac{1}{H_2}\right)\left(-\frac{V_2^2}{X}+\Delta Q_w+Q_w+Q_{s0}\right)\frac{1}{\cos^2\delta}\omega_{12} \\ &\quad -\left(\frac{1}{H_1}+\frac{1}{H_2}\right)\frac{\sin\delta}{\cos\delta}\frac{\Delta Q_w}{T}+\left(\frac{1}{H_1}+\frac{1}{H_2}\right)\frac{\sin\delta}{T\cos\delta}u \\ &= F(\omega_{12},\delta,\Delta Q_w,t)+G(\delta,t)u \end{aligned} \tag{8}$$

where,

$$\begin{aligned}F(\omega_{12},\delta,\Delta Q_w,t) &= -\left(\frac{1}{H_1}+\frac{1}{H_2}\right)\left(\frac{\sin\delta}{\cos\delta}\frac{\Delta Q_w}{T}\right. \\ &\quad \left.-\left(-\frac{V_2^2}{X}+\Delta Q_w+Q_w+Q_{s0}\right)\frac{1}{\cos^2\delta}\omega_{12}\right), \\ G(\delta,t) &= \left(\frac{1}{H_1}+\frac{1}{H_2}\right)\frac{\sin\delta}{T\cos\delta}.\end{aligned}$$

The control objective can be defined as to find the control action u to force the relative rotor speed ω and its first order $\dot{\omega}$ to zero. For the steady state, the relative rotor speed ω_{12} and the reactive power for damping control ΔQ_w are all zeros. So the fixed part $F(0,\delta,0,t)=0$. Most of 2-sliding controllers may be considered as controllers for Eq. (8) steering σ, $\dot{\sigma}$ to 0 in (preferably) finite time. Since Eq.(8) does not remember the original system, such controllers are obviously robust with respect to any perturbations preserving upper and lower bounds. Hence, the problem is to find such a feedback control u that all the trajectories of (8) converge in a finite time to the origin $\sigma=\dot{\sigma}=0$ of the phase plane σ, $\dot{\sigma}$. Thus, based on the fixed gain twisting algorithm [25], the control signal u that can force ω and $\dot{\omega}$ to zero could be selected as

$$u = -r_1\text{sign}(\sigma) - r_2\text{sign}(\dot{\sigma}) \tag{9}$$

with the discontinuous signum function $\text{sign}(\sigma) = \begin{cases} 1, & \sigma > 0 \\ -1, & \sigma < 0 \end{cases}$, where the variables $r_1 > 0$ and $r_2 > 0$ are the control gains. With the above control action, the second order of sliding variable is described by

$$\ddot{\omega}_{12} = F(\omega_{12},\delta,\Delta Q_w,t) + G(\delta,t)(-r_1\text{sign}(\sigma) - r_2\text{sign}(\dot{\sigma})) \tag{10}$$

In order to force ω and $\dot{\omega}$ to zero in a finite time, the control gains should be greater than the magnitude of the uncertainties in F and G. Thus, the control gains r_1 and r_2 should satisfy the [26]

$$(r_1+r_2)K_m - C > (r_1-r_2)K_M + C,\ (r_1-r_2)K_m > C \tag{11}$$

where C should be greater than the maximum value of the $|F|$, with $C \geq |F(\omega,\delta,\Delta Q_w,t)+\Delta F|$. Here, ΔF represents the uncertain part, including the unmolded dynamics and system uncertainties. K_m and K_M are the lower bound and upper bound of G regarding disturbance, respectively, with $K_m \leq G(\delta,t) \leq K_M$.

As shown in (8), if the relative rotor angle δ is an arbitrary variable, the upper bound of G does not exist. However, for an actual power system, the relative rotor angle is relative to the transmission power of a generator and is also related to the static stability [27]. Therefore, the relative rotor angle δ is operated in a limited region. Thus, the upper bound of G exists, and the control gains r_1 and r_2 can be obtained based on the bounds of G and F.

For the wind farm, the reactive power of wind generation has limited rating, $Q_{wmin} \leq Q_w \leq Q_{wmax}$. Thus, the designed control action should be bounded as

$$Q_w - Q_{wmin} \leq u \leq Q_{wmax} - Q_w. \tag{12}$$

The reactive power control order used to damp the system oscillation can be achieved by outer reactive power control loop and inner current control loop as shown in Fig. 2. The reactive power can be controlled by v_{dr}. The v_{dr} and v_{qr} can be controlled using PWM technique via $dq-abc$ transform.

IV. Extension to Multi-Area Power Systems

In this section, a power system with multi-area is considered. The objective is to show how to apply the proposed sliding mode based damping control technique to a multi-area power system. A power system with n machines, l loads and m DFIG based wind farms is considered. For the usual condition, the number of wind farms is less than the number of machines. Although there are $N-1$ oscillation modes in an N areas power system, only a few poorly damping modes are of concern, which are damped using DFIG in this study.

For the multi-area power system, the reduced order nodal admittance matrix can be obtained with the machine buses as

$$I_n = Y_n V_n \tag{13}$$

where $Y_n = G_n + jB_n$.

The injection power of area i can be described as [21]

$$P_i + jQ_i = V_i \sum_{j=1}^{N} V_j(G_{ij} - jB_{ij})(\cos\delta_{ij} + j\sin\delta ij). \tag{14}$$

The swing equation of equivalent machine in each area i is given as [22]

$$\begin{aligned}\dot{\delta}_i &= \omega_i - 1 \\ \dot{\omega}_i &= \frac{1}{H_i}(P_{mi} - P_{ei}) \\ &= \frac{1}{H_i}\left(P_{mi} - V_i\sum_{j=1}^{N} V_j(G_{ij}\cos\theta_{ij} + B_{ij}\sin\theta_{ij})\right)\end{aligned} \tag{15}$$

where the mth wind farm is integrated in area i. The swing equation of the ith area can be rewritten as

$$\dot{\delta}_i = \omega_i - 1$$

$$\dot{\omega}_i = \frac{1}{H_i}(P_{mi} + P_{mw} - P_{ei})$$

$$= \frac{1}{H_i}\left(P_{mi} + P_{mw} - \frac{\Delta Q_{mw} + Q_{mw} + Q_{ms0}}{\sum_{j=1}^{N} V_j(G_{ij}\sin\delta_{ij} - B_{ij}\cos\delta_{ij})} \sum_{j=1}^{N} V_j(G_{ij}\cos\delta_{ij} + B_{ij}\sin\delta_{ij})\right)$$

$$\Delta\dot{Q}_{mw} = \frac{u - \Delta Q_{mw}}{T}. \tag{16}$$

Define that δ_{ij} and ω_{ij} are the relative rotor angle and relative rotor speed of the interarea oscillation, respectively. The mth wind farm involved in the relative system dynamics between areas i and j can be shown as

$$\dot{\delta}_{ij} = \omega_{ij} - 1$$

$$\dot{\omega}_{ij} = \frac{1}{H_i}\left(P_{mi} + P_{mw} - \frac{\Delta Q_{mw} + Q_{mw} + q_{s0}}{\sum_{j=1}^{N} V_j(B_{ij}cos\delta_{ij})} \sum_{k=1}^{N} V_k B_{ik}\sin\delta_{ik}\right) - \frac{1}{H_j}\left(P_{mj} - V_j\sum_{k=1}^{N} V_k B_{jk}\sin\delta_{jk}\right)$$

$$= \frac{1}{H_i}(P_{mi} + P_{mw}) - \frac{1}{H_j}P_{mj} + F(\delta,t) + G(\delta,t)\Delta Q_{mw}$$

$$\Delta\dot{Q}_{mw} = \frac{u - \Delta Q_{mw}}{T_m}. \tag{17}$$

For the mth wind farm, the interarea oscillation between areas i and j can be damped via the proposed sliding mode damping control strategy.

The second-order of sliding variable, $\sigma = \omega_{mij}$ can be obtained as

$$\ddot{\omega}_{ij} = \frac{\partial F(\delta,t)}{\partial\delta_{ij}}\omega_{ij} + \left(\frac{\partial G(\delta,t)}{\partial\delta_{ij}} - \frac{G(\delta,t)}{T_m}\right)\Delta Q_{mw} + \frac{G(\delta,t)}{T_m}u_m$$

$$= F_m(\omega_{ij}, \delta_{ij}, \Delta Q_m, t) + G(\delta_{ij}, t)u_m. \tag{18}$$

Then for the mth wind farm, the sliding mode control based damping control action for the oscillation between areas i and j can be designed using the control law shown in (9).

V. Simulation Study

The time-domain simulations for two different power systems are carried out to illustrate the effectiveness of the designed sliding mode based damping controller for DFIG to mitigate the power system oscillations. In the simulation study, the full order model of DFIG is used. The drive train of DFIG is modeled by a two-mass model.

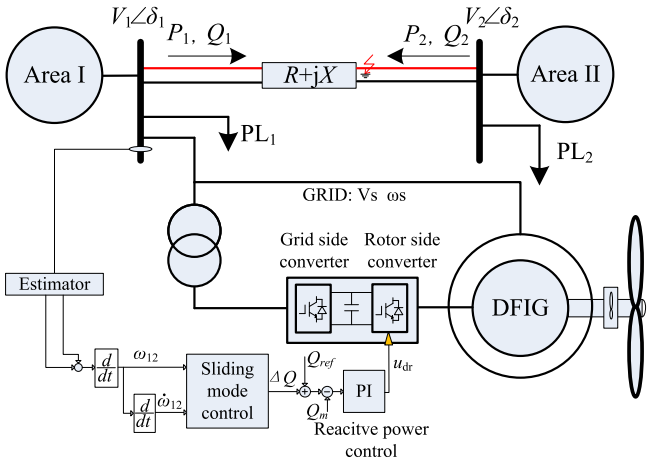

Fig. 4. Two-area power system for simulation.

A. Two-Area Power System

The two-area power system as shown in Fig. 4 is considered firstly. The two areas are connected through a 350 km double ac transmission line with $XL = 0.25\ \Omega$/km, $R = 0.023\ \Omega$/km, and $XC = 12$ nF/km. The transmitted power between the two areas is 260 MW at steady state. A DFIG-based wind farm represented by one aggregated DFIG is connected to the grid in Area I. The wind farm is equivalent by a DFIG with coordinated rate. The size of wind farm is leveled to achieve that the wind penetration level in the whole system is 10% when the wind farm is at its rated output. The rated reactive power of DFIG is 0.5 p.u. and the regulation bounds are ± 0.1 p.u. The designed parameters of the sliding mode damping controller are shown in the Appendix.

Two three-phase faults occur at the midpoint of the transmission line and 10 km away from Bus 1 are simulated respectively. These faults occur at $t = 1$ s and are cleared after 0.05 s. The interarea oscillation is caused by this fault. The designed sliding mode based damping controller is then activated in response to the rotor angle difference estimated at bus 1. The damping controller modulates the reactive power of DFIG to damp the power oscillation rapidly.

The transient responses of the system when DFIG is with and without damping controller are shown in Figs. 5 to 8. The dynamic behaviors of synchronous machines are shown in Figs. 5 and 7. The transient responses of the DFIG after the fault are given in Figs. 6 and 8.

The curves in these figures show that the system with bad damping and the oscillation lasts a long time in the scenario without damping controller added to DFIG. Due to the decoupled control strategy from the grid, the reactive power and active power of DFIG will utmost keep its order value when the fault occurs. As the dotted lines in Figs. 6 and 8 shown, there are

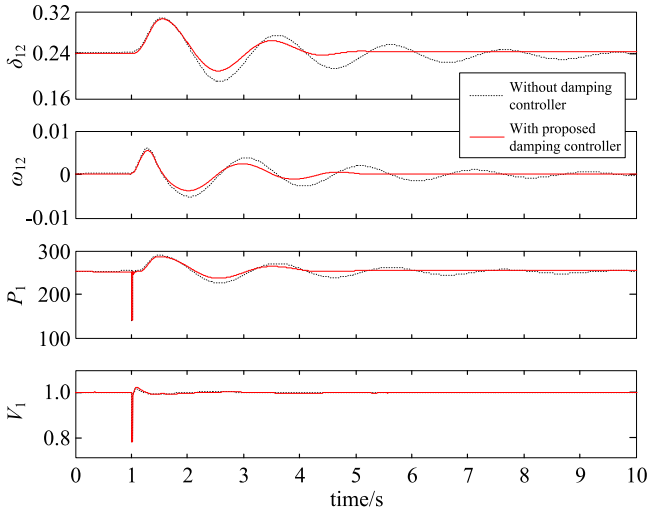

Fig. 5. The dynamic response of two-area power system for the midpoint fault. (a) Relative rotor angle. (b) Relative rotor speed. (c) Transmitted active power between the two areas. (d) Voltage of bus 1.

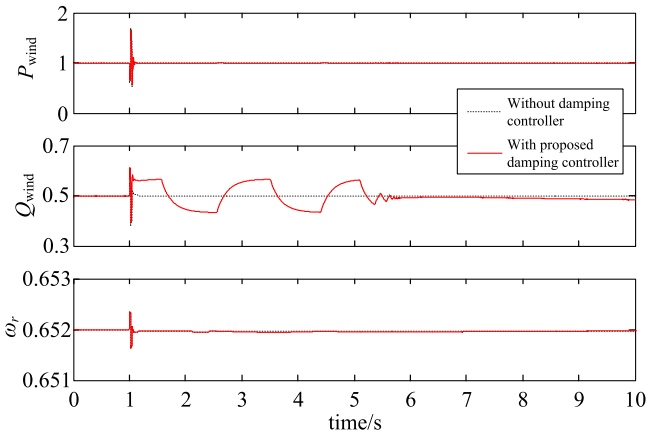

Fig. 6. The dynamic response of DFIG for the midpoint fault. (a) Active power. (b) Reactive power. (c) Rotor speed.

almost no changing of output power of DFIG after the faults are cleared in the scenario without additional damping controller.

As the solid lines in Figs. 5 and 7 shown, when the proposed sliding mode damping controller is applied to the DFIG, the proposed damping controller effectively damps the interarea power oscillation caused by the line fault.

Since the sliding mode damping controller is added to the reactive power control loop of DFIG, the modulated reactive power of DFIG is injected into the system to damp oscillations. The dynamic response of the DFIG also illustrates that the proposed damping control strategy has almost no influence on DFIG active power output and shaft torque, as shown in Figs. 6 and 8.

Although the sliding mode damping controller is designed based on the reduced-order model of DFIG, the simulation on a full-order model indicates that the proposed controller is capable of dealing with the uncertainty caused by unmodeled part.

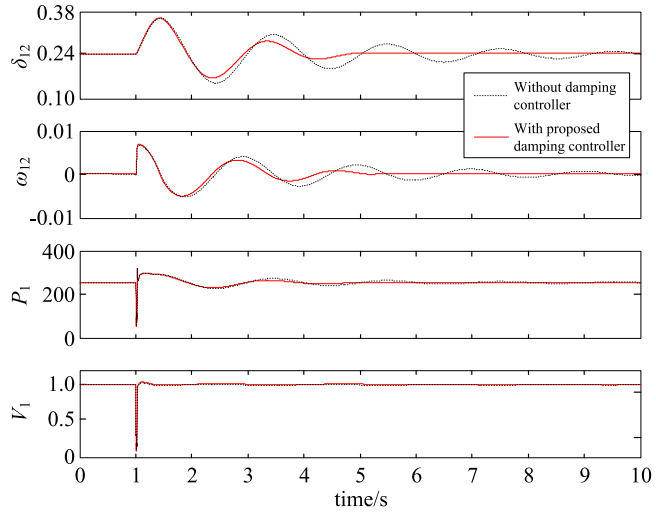

Fig. 7. The dynamic response of two-area power system for 10km fault. (a) Relative rotor angle. (b) Relative rotor speed. (c) Transmitted active power between the two areas. (d) Voltage of bus 1.

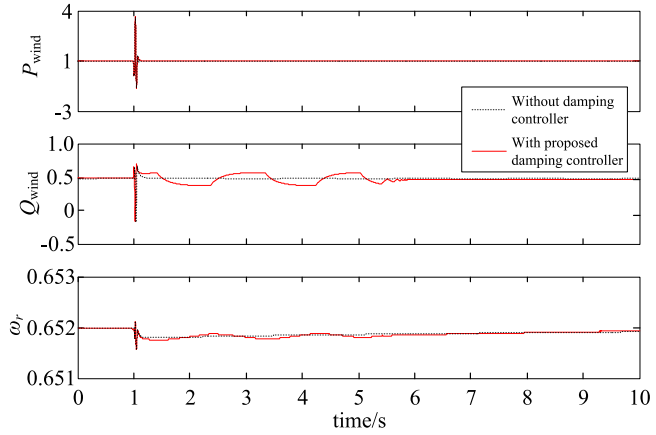

Fig. 8. The dynamic response of DFIG for a fault 10 km away from Bus 1. (a) Active power. (b) Reactive power. (c) Rotor speed.

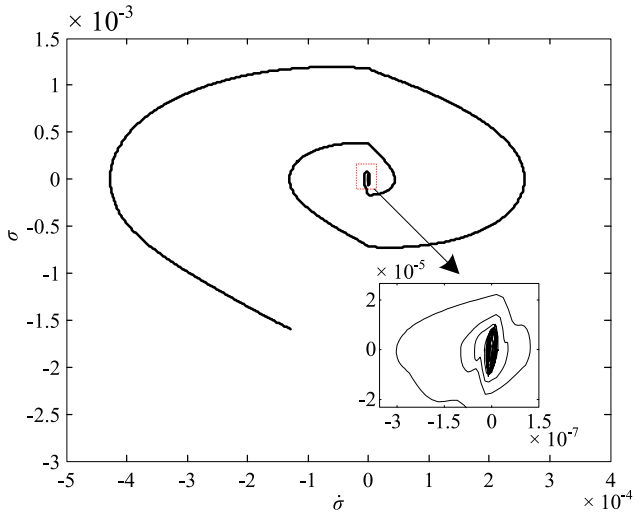

Fig. 9. $\sigma - \dot{\sigma}$ phase trajectory.

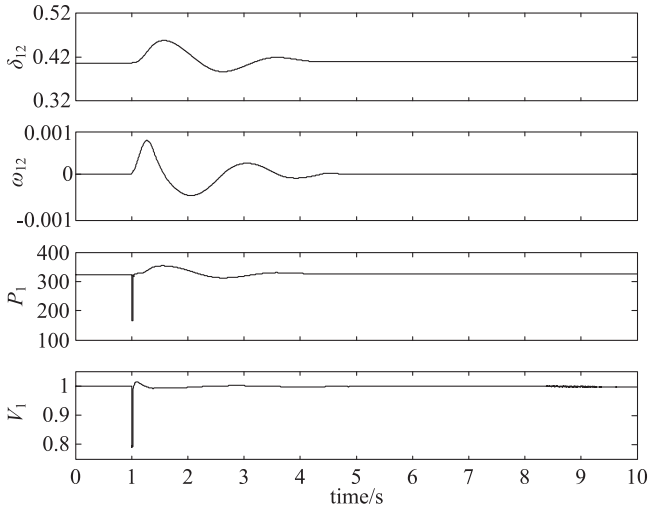

Fig. 10. The system dynamic response of the increased transmitted power scenario, with proposed damping controller.

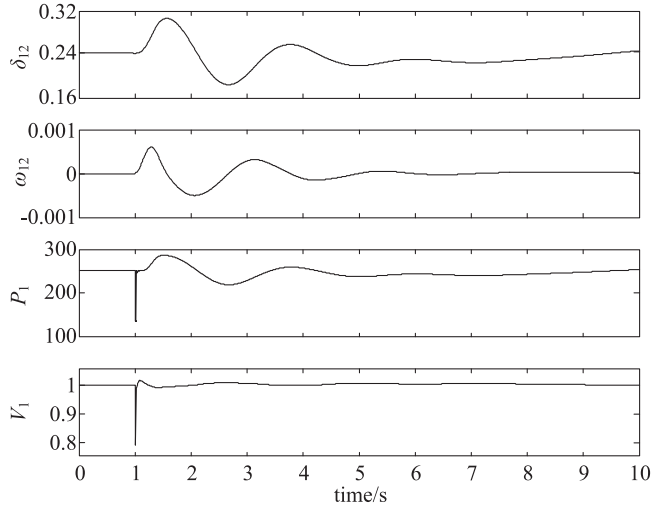

Fig. 11. The system dynamic response of the initial transmitted power scenario, with conventional damping controller.

Illustratively, Fig. 9 gives the phase trajectory of the power system in the state space ($\sigma - \dot{\sigma}$ plane). It can be seen that the controlled system converged to the sliding surface with the sliding variable and its first-order both equal to zero.

In order to illustrate the robustness of the proposed sliding mode damping control with regard to the ranging of operation points, the simulation with a heavier load scenario is carried out. In this simulation scenario, the transmitted power between area I and area II is increased from 260 MW to 320 MW. With the same second-order sliding mode damping control and parameters, the dynamic response of the heavier load scenario system is plotted in Fig. 10. As shown, the oscillation is damped quickly. It illustrates that the proposed sliding mode damping control is robust to the system operation point changing.

In addition, a comparison is carried out to the one with conventional damping control, which is designed based on the small signal linearization algorithm with respect to one operation point, as introduced in [5]. The parameters of the conventional damping controller for DFIG is designed based on the operation point of the initial scenario, with 260 MW transmitted power between the two areas. The dynamic responses in 260 MW transmitted power scenario and 260 MW transmitted power scenario are shown in Figs. 11 and 12, respectively.

As shown in Fig. 11, the conventional damping controller is efficient in damping the system oscillation in the initial scenario (with 260 MW transmitted power). However, as the operation point changed (with 320 MW transmitted power), the conventional damping controller becomes less efficiently in damping the oscillation, as shown in Fig. 12. Comparing the dynamic responses given in Figs. 10 and 12, it is clear to show that the proposed second-order sliding mode damping controller is much more robust than the conventional damping control with respect to the various operation points.

B. 10-Machine 39-Bus Power System

The proposed sliding mode damping controller is tested in a more practical situation to demonstrate the effectiveness. The

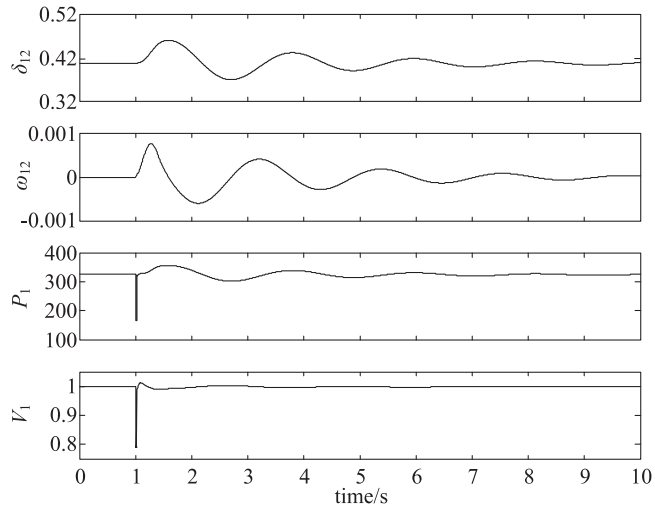

Fig. 12. The system dynamic response of the increased transmitted power scenario, with conventional damping controller.

proposed controller is applied to a 10-machine 39-bus power system [28]. The structure of the study system is shown in Fig. 13. Two DFIG based wind farms are considered in this system. One is connected at bus 39 and another is connected at bus 35. In this system, generator 1 connected at bus 31 is selected as the slack generator.

In this case, a three-phase line fault between bus 4 and bus 14 occurs at $t = 1$ s and is cleared after 0.1 s. For the wind farm connected at bus 39, the angle difference between G2 and G10 is employed as the input data for sliding mode damping controller. Similarly, for the wind farm connected at bus 35, the angle difference between G6 and G7 is employed as the input data for sliding mode damping controller.

The dynamic behaviors of the synchronous machines are shown in Figs. 14, 15 and 16 in the scenario without damping controller. Fig. 14 shows the dynamic responses of relative rotor angle of G2-G10. Fig. 15 shows the dynamic responses

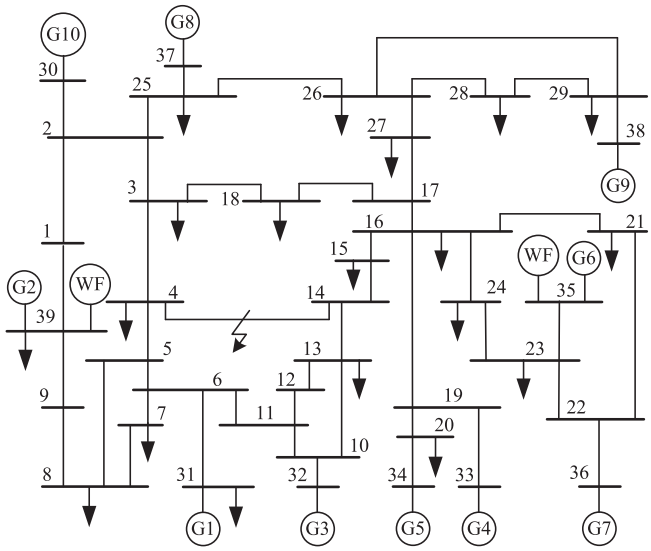

Fig. 13. The structure of the multi-area power system.

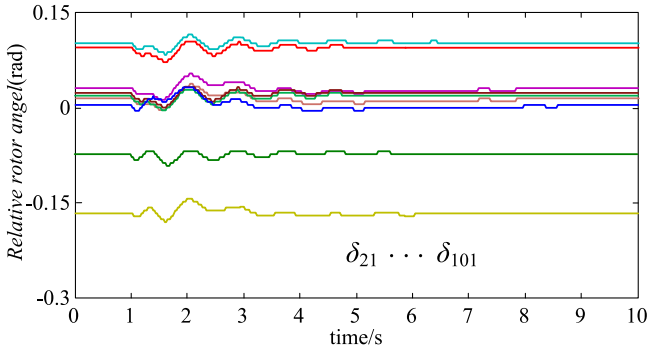

Fig. 14. The dynamic response of relative rotor angle of synchronous machines in the scenario without damping controller.

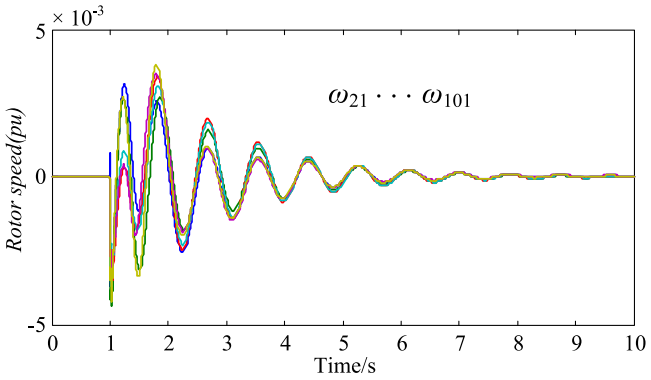

Fig. 15. The dynamic response of relative rotor speed of synchronous machines in the scenario without damping controller.

of relative rotor speed of G2-G10. Fig. 16 gives the dynamic responses of bus voltages. The dynamic responses of the two DFIG based wind farms are shown in Fig. 17.

The dynamic behaviors of the synchronous machines in the sliding mode damping controller scenario are shown in Figs. 18, 19 and 20. Fig. 18 demonstrates the dynamic responses of relative rotor angle of G2-G10. Fig. 19 displays the dynamic responses of relative rotor speed of G2-G10. Fig. 20 gives the dynamic responses of bus voltages. The dynamic responses of the two DFIG based wind farms are shown in Fig. 21.

It can be seen that compared to the scenario without damping controller, the system power oscillations are damped more quickly. The simulation results illustrate that the proposed slid-

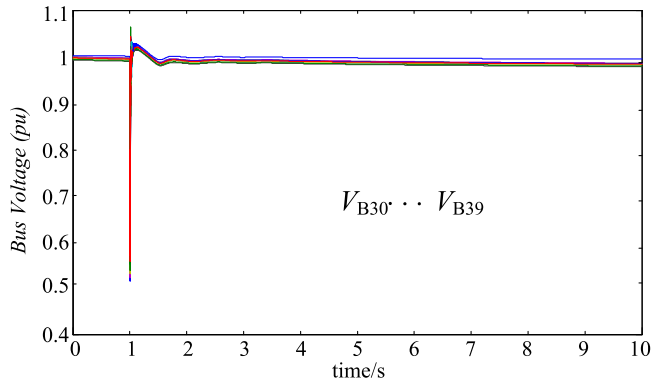

Fig. 16. The dynamic response of bus voltages in the scenario without damping controller.

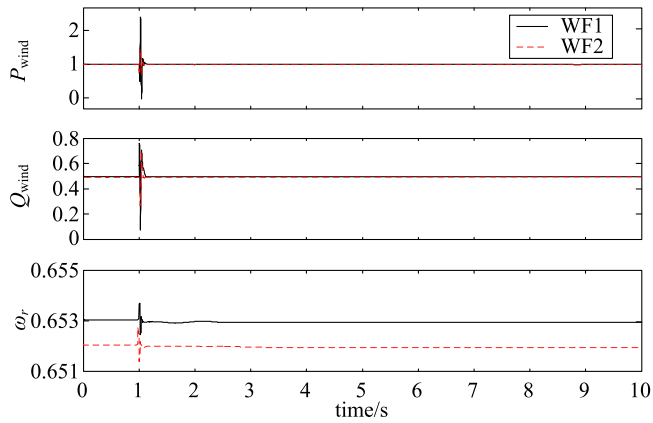

Fig. 17. The dynamic response of DFIG based wind farms in the scenario without damping controller. From top to bellow: active power, reactive power, rotor speed.

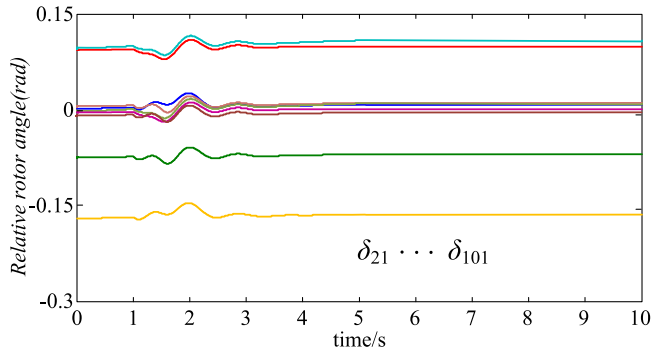

Fig. 18. The dynamic response of relative rotor angle of synchronous machines in the scenario with proposed damping controller.

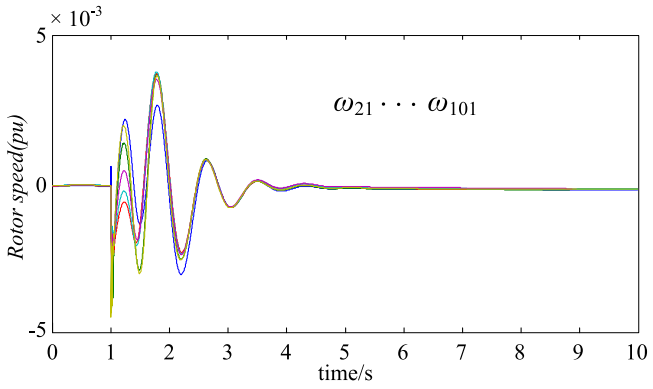

Fig. 19. The dynamic response of relative rotor speed of synchronous machines in the scenario with proposed damping controller.

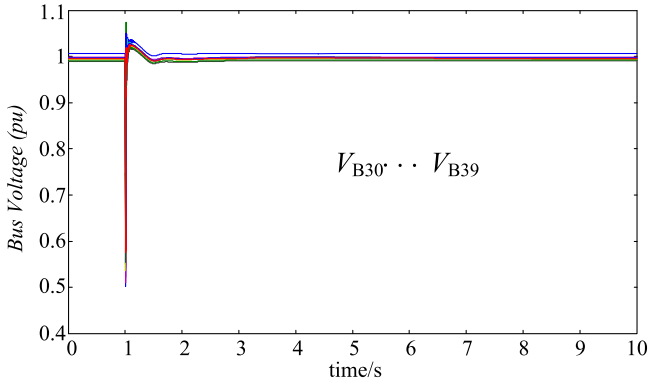

Fig. 20. The dynamic response of bus voltages in the scenario with proposed damping controller.

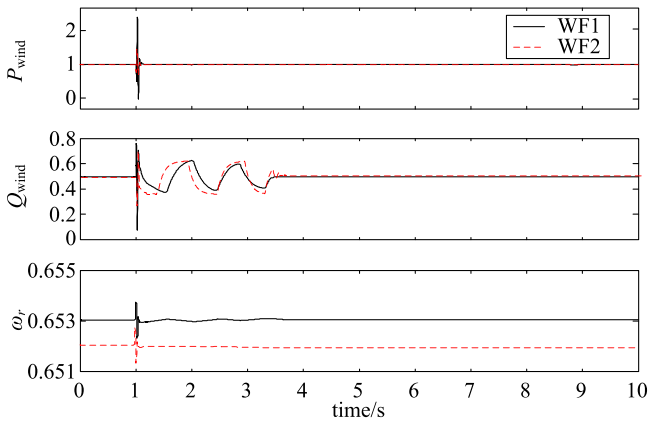

Fig. 21. The dynamic response of DFIG based wind farms in the scenario with damping controller. From top to bellow: active power, reactive power, rotor speed.

ing mode damping control installed on DFIG is effective to damp the oscillation modes.

VI. Conclusion

In this paper, a second-order sliding mode based damping controller is proposed for DFIG against interarea oscillations in a multiple areas transmission system. The proposed damping controller allows the DFIG based wind farm to modulate its output reactive power, thereby enhancing the damping of power system and stabilizing the system force to the disturbances. Specifically, the second-order sliding mode is employed to design the control law. Thus, the control action will not require a discrete reactive power output of DFIG. Compared with conventional controllers, the proposed damping controller is advanced in the high degree robustness to the system uncertainties and system unmolded dynamics, meaning that it can enhance the system stability in a wide range of operation points and system parameters. The analyses and simulations are carried out on a two-area power system and a multi-area power system. The simulation results have demonstrated the effectiveness and robustness of the proposed damping controller.

TABLE I
Parameters of DFIG

Stator resistance, $r_s\,(pu)$	0.007
Stator inductance, $L_{ls}\,(pu)$	0.18
Mutual inductance, $L_m\,(pu)$	2.9
Rotor resistance, $R_r\,(pu)$	0.005
Rotor inductance, $L_{lr}\,(pu)$	0.156
Coupling inductor inductance, $L(pu)$	0.00178
Coupling inductor resistance, $R(pu)$	0.000929
Proportion of PI controller for outer loop, K_{po}	0.002
Integration of PI controller for outer loop, K_{io}	0.05
Proportion of PI controller for inner loop, K_{pi}	0.03
Integration of PI controller for inner loop, K_{ii}	0.5

Appendix A

The parameters of DFIG are listed in Table I.

The parameters of the designed sliding mode damping controller is given below:

For two-area power system: $r_1 = 0.1$; $r_2 = 0.02$;

For multi-area power system: WF1:$r_1 = 0.12$; $r_2 = 0.02$; WF2: $r_1 = 0.1$; $r_2 = 0.01$;

References

[1] *Global Wind Energy Outlook 2012*, Wind Energy Council. Burssels, Belgium, 2012.

[2] G. Abad, J. Lopez, M. Rodriguez, L. Marroyo, and G. Iwanski, *Doubly Fed induciton Machine.* Hoboken, NJ, USA: Wiley, 2011.

[3] S. Muller, M. Deicke, and R. W. De Doncker, "Doubly fed induction generator systems for wind turbines," *IEEE Ind. Appl. Mag.*, vol. 8, no. 3, pp. 26–33, Jun. 2002.

[4] P. Kundur, *Power System Stability and Control.* New York, NY, USA: McGraw-Hill, 1994.

[5] L. P. Kunjunmuhammed, B. C. Pal, C. Oates, and K. J. Dyke, "Electrical oscillations in wind farm systems: Analysis and insight based on detailed modeling," *IEEE Trans. Sustainable Energy*, vol. 7, no. 1, pp. 51–62, Jan. 2016.

[6] M. Edrah, K. L. Lo, and O. Anaya-Lara, "Impacts of high penetration of DFIG wind turbines on rotor angle stability of power systems," *IEEE Trans. Sustainable Energy*, vol. 6, no. 3, pp. 759–766, Jul. 2015.

[7] F. M. Hughes, O. Anaya-Lara, N. Jenkins, and G. Strbac, "A power system stabilizer for DFIG-based wind generation," *IEEE Trans. Power Syst.*, vol. 21, no. 2, pp. 763–C772, May 2006.

[8] Z. Miao, L. Fan, D. Osborn, and S. Yuvarajan, "Control of DFIG-based wind generation to improve interarea oscillation damping," *IEEE Trans. Energy Convers.*, vol. 24, no. 2, pp. 415–C422, Jun. 2009.

[9] Y. Tang, H. He, J. Wen, and J. Liu, "Power system stability control for a wind farm based on adaptive dynamic programming," *IEEE Trans. Smart Grid*, vol. 6, no. 1, pp. 166–177, Jan. 2015.

[10] M. Singh, A. J. Allen, E. Muljadi, V. Gevorgian, Y. Zhang, and S. Santoso, "Interarea oscillation damping controls for wind power plants," *IEEE Trans. Sustainable Energy*, vol. 6, no. 3, pp. 967–975, Jul. 2015.

[11] G. Tsourakis, B. M. Nomikos, and C. D. Vournas, "Contribution of doubly fed wind generators to oscillation damping," *IEEE Trans. Energy Convers.*, vol. 24, no. 3, pp. 783–C791, Sep. 2009.

[12] A. Mitra and D. Chatterjee, "Active power control of DFIG-based wind farm for improvement of transient stability of power systems," *IEEE Trans. Power Syst.*, vol. 31, no. 1, pp. 82–93, Jan. 2014.

[13] M. Mokhtari and F. Aminifar, "Toward wide-area oscillation control through doubly-fed induction generator wind farms," *IEEE Trans. Power Syst.*, vol. 29, no. 6, pp. 2985–2992, Nov. 2014.

[14] Y. Mishra, S. Mishra, F. Li, Z. Y. Dong, and R. C. Bansal, "Small-Signal Stability Analysis of a DFIG-Based Wind Power System Under Different Modes of Operation," *IEEE Trans. Energy Convers.*, vol. 24, no. 4, pp. 972–982, Dec. 2009.

[15] Y. Mishra, S. Mishra, M. Tripathy, N. Senroy, and Z. Y. Dong, "Improving stability of a DFIG-based wind power system with tuned damping controller," *IEEE Trans. Energy Convers.*, vol. 24, no. 3, pp. 650–C660, Sep. 2009.

[16] L. Yang, G. Y. Yang, Z. Xu, Z. Y. Dong, K. P. Wong, and X. Ma, "Optimal controller design of a doubly-fed induction generator wind turbine system for small signal stability enhancement," *IET Generation, Transmiss. Distrib.*, vol. 4, no. 5, pp. 579–597, Dec. 2009.

[17] Y. Tang, P. Ju, H. He, C. Qin, and F. Wu, "Optimized control of DFIG-based wind generation using sensitivity analysis and particle swarm optimization," *IEEE Trans. Smart Grid*, vol. 4, no. 1, pp. 509–520, Nov. 2013.

[18] T. Surinkaew and I. Ngamroo, "Coordinated robust control of DFIG wind turbine and PSS for stabilization of power oscillations considering system uncertainties," *IEEE Trans. Sustainable Energy*, vol. 5, no. 3, pp. 51–62, Jul. 2014.

[19] L. Fan, H. Yin, and Z. Miao, "On active/reactive power modulation of DFIG-based wind generation for interarea oscillation damping," *IEEE Trans. Energy Convers.*, vol. 26, no. 2, pp. 513–521, 2011.

[20] F. Pourboghrat, F. Farid, C. J. Hatziadoniu, M. Daneshdoost, F. Mehdian, and M. Lotfalian, "Local sliding control for damping interarea power oscillations," *IEEE Trans. Power Syst.*, vol. 19, no. 2, pp. 1123–1134, May 2004.

[21] A. R. Bergen, *Power Systems Analysis*. Englewood Cliffs, NJ, USA: Prentice-Hall, 1986.

[22] P. M. Anderson and A. A. Foad, *Power System Control and Stability*. New York, NY, USA: IEEE Press, 1994.

[23] T. J. E. Miller, *Reactive Power Control in Electric Systems*. New York, NY, USA: Wiley, 1982.

[24] H. Nguyen-Duc, Louis-A Dessaint, A. F. Okou, and I. Kamwa, "A power oscillation damping control scheme based on bang-bang modulation of FACTS signals," *IEEE Trans. Power Syst.*, vol. 25, no. 4, pp. 1918–1927, Nov. 2010.

[25] A. Levant, "Sliding order and sliding accuracy in sliding mode control," *Int. J. Control*, vol. 58, no. 6, pp. 1247–1263, Nov. 1993.

[26] A. Levant, "Principles of 2-sliding mode design," *Automatica*, vol. 43, no. 4, pp. 576–586, Oct. 2007.

[27] L. Yang, Z. Xu, J. Ostergaard, Z. Y. Dong, K. P. Wong, and X. Ma, "Oscillatory stability and eigenvalue sensitivity analysis of a dfig wind turbine system," *IEEE Trans. Energy Convers.*, vol. 26, no. 1, pp. 328–339, Feb. 2011.

[28] A. Pai, *Energy Function Analysis for Power System Stability*. New York, NY, USA: Springer, 1989.

Kai Liao received the B.Sc. degree in electrical engineering in 2011, from Southwest Jiaotong University, Chengdu, China, where he is currently working toward the Ph.D. degree in electrical engineering.

His research interests include power system stability analysis and wind energy.

Zhengyou He (M'10–SM'14) was born in Sichuan Province, China, in 1970. He received the B.Sc. and M.Sc. degrees in computational mechanics from Chongqing University, Chongqing, China, in 1992 and 1995, respectively, and the Ph.D. degree in electrical engineering from Southwest Jiaotong University, Chengdu, China, in 2001.

Since 2002, he has been a Professor in the Department of Electrical Engineering, Southwest Jiaotong University. His research interests include the area of signal processing and information theory and its application in electrical power systems and the application of wavelet transforms in power systems.

Yan Xu (S'10–M'13) received the B.E. and M.E. degrees from the South China University of Technology, Guangzhou, China, in 2008 and 2011, and the Ph.D. degree in electrical engineering from the University of Newcastle, Callaghan, Australia, in 2013.

From 2013 to 2014, he was a Research Fellow with the Center for Intelligent Electricity Networks, University of Newcastle. He is currently a Post Doctoral Fellow in the School of Electrical and Information Engineering, University of Sydney, Sydney, Australia. His research interests include power system stability and control, power system planning, smart grid, and intelligent system applications to power engineering.

Guo Chen (M'10) received the Ph.D. degree in electrical engineering from the University of Queensland, Brisbane, Australia, in 2010. He is now a Research Fellow at the School of Electrical Engineering and Computer Science, the University of Newcastle, Australia. Previously, he was a Research Fellow at the Australian National University and the University of Sydney, Australia. He is the recipient of the Australian Research Council Discovery Early Career Researcher Award in 2015. His research interests include optimization and control, complex network, dynamical systems, intelligent algorithms and their applications in smart grid.

Zhaoyang Dong (M'99–SM'06) received the Ph.D. degree in electrical engineering from the University of Sydney, Sydney, Australia, in 1999. He is currently a Professor and the Head of the School of Electrical and Information Engineering, University of Sydney. He is the Immediate Ausgrid Chair and Director of the Centre for Intelligent Electricity Networks, University of Newcastle, Callaghan, Australia. He previously held academic and industrial positions with the Hong Kong Polytechnic University, Hong Kong, and Transend Networks (now TasNetworks), Tasmania, Australia. His research interests include smart grid, power system planning, power system security, load modeling, electricity market, and computational intelligence and its application in power engineering.

Kit Po Wong (M'87–SM'90–F'02) received the M.Sc, Ph.D. and D.Eng. degrees from the Institute of Science and Technology, University of Manchester, Manchester, U.K., in 1972, 1974 and 2001, respectively. Since 1974, he has been with the School of Electrical, Electronic and Computer Engineering, University of Western Australia, Perth, Australia, where he is currently a Winthrop Professor. From 2002 to 2011, he was also with Department of Electrical Engineering, Hong Kong Polytechnic University, as a Chair Professor and the Head from 2002 to 2007. He is a Con-joint Professor of The University of Newcastle, Australia. His current research interests include power system analysis, planning and operations, smart grids and renewable energy.

He received three Sir John Madsen Medals in 1981, 1982, and 1988, respectively, from the Institution of Engineers Australia, the 1999 Outstanding Engineer Award from IEEE Power Chapter Western Australia, and the 2000 IEEE Third Millennium Award. He was a Co-Technical Chairman of IEEE Machine Learning and Cybernetics 2004 Conference and the General Chairman of IEEE/CSEE PowerCon2000. He is currently the Editor-in-Chief of IEEE POWER ENGINEERING LETTERS and was the Editor-in-Chief of IEE Processing Generation, Transmission & Distribution. He is a Fellow IET, HKIE, and IEAust.